L-Band Wavelength-Tunable MQW Fabry−Pérot Laser Using a Three-Segment Structure

Ke Liu, Si Xuan Mu, Yu Lu, Bao Lu Guan, and Edwin Yue Bun Pun

***Abstract*— A three-segment structure L-band wavelength tunable multi-quantum-well Fabry–Pérot (FP) laser is realized and characterized. Wavelength-tuning is achieved by current injection into the unpumped segments. Depending on the pumping schemes, the lasing wavelength undergoes either red or blue shift. Red-shifting of the lasing wavelength is caused by band-gap shrinkage effect because of Joule heating. Blue-shifting of the lasing wavelength is mainly caused by band-gap filling effect. At room temperature, a tuning range of ∼12.8 nm is obtained. The tunable FP laser diode with simple architecture has potential applications in L-band optical communication systems.**

***Index Terms*— Fabry−Pérot laser, wavelength-tunable, band-gap shrinkage, band-gap filling, optical waveguide.**

I. Introduction

OPTICAL transmission in the L-band wavelength (1565 nm−1625 nm) extends the available bandwidth of wavelength division multiplexing system, and thereby increases the network capacity and flexibility [1]. Wavelength-tunable semiconductor lasers have attracted great interest as light sources used in optical networks and sensing systems. The field of tunable lasers is diverse and a number of interesting device concepts have been proposed and demonstrated [2], [3]. The tunability can be understood basically as a gain generating medium plus one or more tuning sections. Considering the configurations of tunable lasers, the technologies are mainly divided into two categories, namely monolithic integrated lasers [4] and external cavity lasers [5]. Electrical tuning is one of the simplest and reliable techniques in the former category, e.g., a tunable Fabry−Pérot (FP) laser based on a two-section slotted structure on a ridge laser using Vernier effect [6]. A two-section tunable InGaAsP/InP FP laser was also demonstrated using different current density ratios between the two sections [7]. Partially pumped semiconductor waveguide lasers having an unpumped segment were realized in both GaAs-based materials [8], [9] and InGaAsP/InP materials [10]. The unpumped segment within the laser cavity acts as a saturable absorber and is used for wavelength tuning. Recently, a three-section slotted FP laser was demonstrated [11], and only the laser system transmission properties were studied. However, the mechanisms of wavelength shift depend on the semiconductor material, and few full investigations on the structure with active/passive segments have been reported.

In this letter, a L-band wavelength-tunable multi-quantum well (MQW) FP laser using a three-segment structure is realized and characterized. The structure uses three separate metal-contact electrodes that provide individually driving current for each segment. Wavelength-tuning is achieved by current injection into the unpumped segments. The wavelength tunability is studied in the case of partially/entirely pumped laser as a function of current density, different pump configurations of the electrodes, and at different submount temperatures, respectively. The corresponding mechanisms of lasing wavelength shifts are discussed.

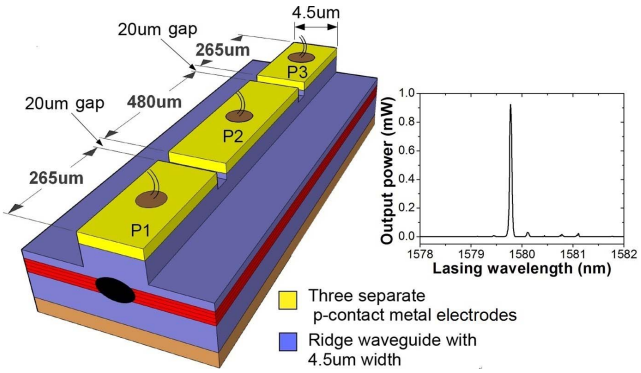

Fig. 1. A schematic top-view of a MQW FP laser with three p-contact metal electrodes separated by isolation gaps of 20 μm width. Inset shows a typical lasing spectrum with one single longitudinal mode; the P1 segment was pumped with a current of 138 mA, and the P3 segment serves as a tuning section and was pumped with a current of 10 mA.

II. Experimental

Fig. 1 shows a schematic top-view of the three-segment structure MQW FP laser with three p-contact metal electrodes indicated by P1, P2, and P3, and the corresponding segment length is 265 μm, 480 μm, and 265 μm, respectively. The electrodes were separated by isolation gaps of 20 μm width. In order to isolate electrically the laser into three segments, the metal electrode and the highly doped GaInAs contact layers were removed in the gaps. The electrode to electrode resistance was measured to be >1.0 KΩ. Inset shows a typical lasing spectrum with one single longitudinal mode;

Manuscript received March 26, 2013; revised May 20, 2013; accepted June 17, 2013. Date of publication July 19, 2013; date of current version August 16, 2013. This work was supported in part by the Importation and Development of High-Caliber Talents Project of Beijing Municipal Institutions, China under Grant 002000543113508, in part by the Scientific Research Foundation for the Scholars with the Ph.D. degree, Beijing University of Technology, China under Grant 002000543112533.

K. Liu, S. X. Mu, Y. Lu, and B. L. Guan are with the Key Laboratory of Optoelectronics Technology, Ministry of Education, Beijing University of Technology, Beijing 100124, China (e-mail: liuke@bjut.edu.cn; liukcityu@yahoo.com).

E. Y. B. Pun is with the Department of Electronic Engineering, City University of Hong Kong, Hong Kong.

Color versions of one or more of the figures in this letter are available online at http://ieeexplore.ieee.org.

Digital Object Identifier 10.1109/LPT.2013.2273367

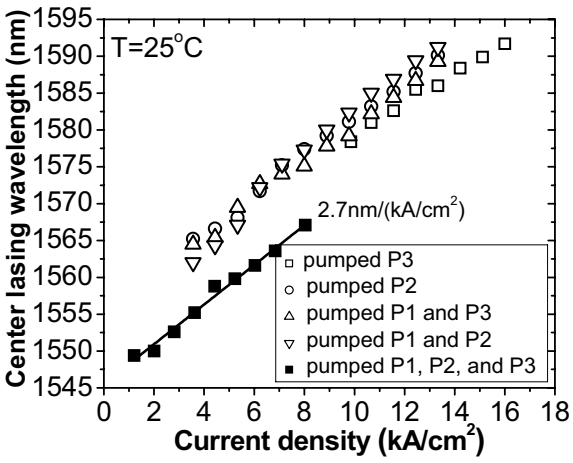

Fig. 2. Dependence of center lasing wavelength on current density for different electrode pump configurations under a constant submount temperature of 25 °C.

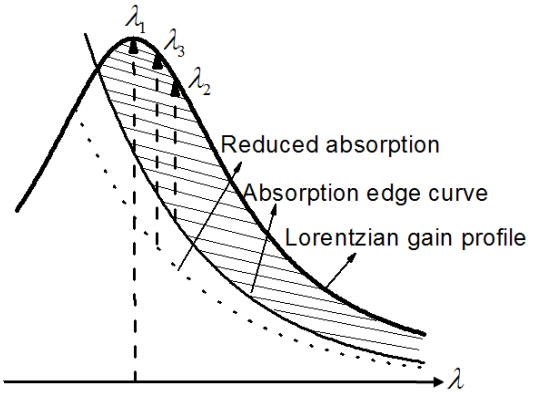

Fig. 3. Schematic diagram showing the lasing wavelength selection for device with partially/entirely pumped segments. λ_1: lasing wavelength of an entirely pumped laser (P1 + P2 + P3 pumped), λ_2: lasing wavelength of a partially pumped laser (P2 or P3 pumped, P1 + P2 or P1 + P3 pumped), λ_3: lasing wavelength of a partially pumped laser with current injection into the unpumped segment (P1 pumped).

the P1 segment pumped with a current of 138 mA, and the unpumped P2 segment becomes an absorber, while the P3 segment serves as a tuning section and was pumped with a current of 10 mA.

The ridge waveguide laser was fabricated on InP substrate using a MQW epitaxial structure. A typical photoluminescence (PL) peak from these QW materials is located at ~1545 nm wavelength at room temperature. Standard photolithographic, metallization, and bonding techniques were used in the processing of these devices. The ~4.5 μm wide waveguides were reactive ion etched using an Oxford PlasmaLab 100 ICP system to a depth of ~1.4 μm to ensure single mode operation. The device was attached to a submount with p-side up, and each segment could be driven individually using ILX Lightwave LDC-3724B laser diode driver controllers. The submount temperature was controlled by a thermoelectric cooler underneath a copper cold-plate with a thermistor inside. The lasing spectrum of these waveguide laser diodes under continuous-wave operation was measured using an Agilent 86140B optical spectrum analyzer. Single longitudinal mode is observed in these tunable FP lasers under different operation conditions carried out, as shown in the inset of Fig. 1.

III. Results and Discussion

Fig. 2 shows the center lasing wavelength shift as a function of current density for different pumped configurations of the electrodes under a constant submount temperature of 25 °C. When the two adjacent segments (e.g. P1 and P2) or the entire pumped segments are pumped, these segments exhibit similar current densities for lasing. The center lasing wavelength in each case all shows a red-shift with increasing current density. This shift is mainly due to the band-gap shrinkage effect, where the energy of the conduction band edge becomes lower. The effect caused by Joule heating in the active region shifts the peak wavelength of the cavity gain profile to longer wavelength. Therefore, the instantaneous rising temperature resulting from higher current density in the QW regions changes the refractive index of the QW materials and the effective cavity length of the laser. A wavelength-tuning coefficient versus current density is measured to be ~2.7 nm/(kA/cm^2), by a linear fit in the case of entirely pumped segments. Similar coefficient values are also obtained for the other cases. The output powers of these lasers usually fluctuate as the driving current is increased. In the case of entirely pumped laser, the lasing power is in the range 1.12 mW to 1.36 mW. When the laser cavity has an unpumped segments, the power is usually lower than that of the case of entirely pumped segments with a similar level of current density. For the laser with pumped P3 segment, the output power is in the range 0.82 mW to 1.08 mW.

Comparing the center lasing wavelength with similar current density, partially pumped laser (with any unpumped segments) exhibits a red-shift in comparing to an entirely pumped laser. When an unpumped segment is introduced within the cavity and its length is comparable to or longer than the pumped segment, the unpumped segment becomes an absorber. Without the temperature effect light near the band-gap wavelength should lase after above threshold current is injected into the pumped segment. However, since the absorber exhibits large absorption at this wavelength of light, the lasing condition is difficult to satisfy. In practice, increasing the current injection leads to larger heat generation in the QW regions, and this tends to shrink the band-gap and lower the energy of light that can lase. Also, the absorption tends to decrease at lower energy of light since its temperature is lower than that of the pumped region. Fig. 3 shows a schematic diagram of the lasing wavelength selection for laser with partially/entirely pumped segments, and a Lorentzian gain profile is usually assumed for the gain medium of semiconductor material. The absorption edge of the material in the unpumped segment is blue-shifted, and the lasing wavelength should occur in the shaded region. The absorption coefficient α is expressed as a function of photon energy hν following the Urbach's rule [12]

$$\alpha(h\nu) = \alpha_0 \exp[-\sigma(E_0 - h\nu)/k_B T] \quad (1)$$

where α_0 and E_0 are the characteristic parameters of the material, σ is the steepness parameter, k_B is the Boltzmann

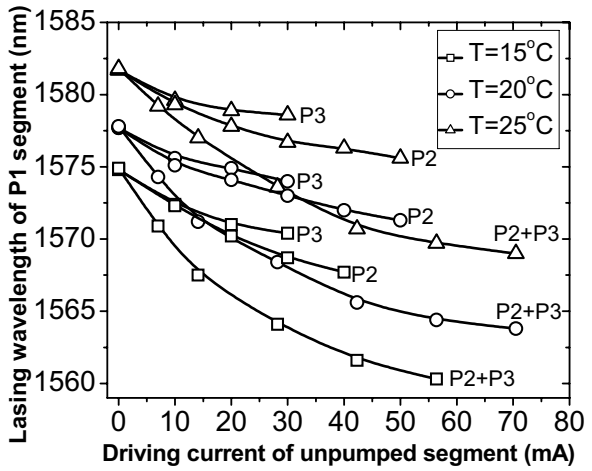

Fig. 4. Wavelength tuning (with P1 segment pumped above threshold) as a function of current injection into the previously unpumped segments (P2, P3 or P2 + P3) of the laser at various submount temperatures.

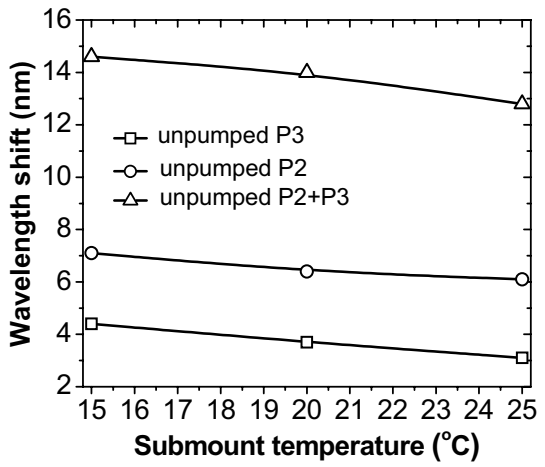

Fig. 5. Total wavelength shift as a function of temperature with P1 segment pumped above threshold and P2, P3, or P2 + P3 segment as a tuning section.

constant, and T is the temperature. Eq. (1) indicates that the absorption edge of semiconductor materials varies exponentially with energy. The effective gain profile G(hν) and the modal absorption spectrum α(hν) are related by [13]

$$G(h\nu) = \alpha(h\nu)[f_c(E_1, E_{fc}) - f_v(E_2, E_{fv})] \qquad (2)$$

where the transition energy is given by h$\nu = \mathrm{E_1}-\mathrm{E_2}$. The gain and absorption coefficients are taken as positive quantities, and f_c and f_v are the Fermi factors controlling the occupancy of the conduction and valence band states, respectively. Eq. (2) shows that the gain profile is related closely to the absorption spectrum, especially in the unpumped segment, where the absorption loss is larger. In this case, the effective gain profile of the composite cavity peaks at a longer wavelength (e.g., λ_2 in Fig. 3) in comparison with the band-gap wavelength of the pumped segment (e.g., λ_1 in Fig. 3). It is well known that in an edge-emitted laser the lasing wavelength is almost equivalent to the gain peak wavelength. As a result, the lasing wavelength for the composite cavity shows a red-shift compared with that of the cavity without any unpumped segment, as shown in Fig. 2.

Fig. 4 shows the lasing wavelength tuning of the laser (with P1 segment pumped above threshold) as a function of current injection into the previously unpumped segments at various submount temperatures. A constant driving current of 138 mA (or J = 11.6 kA/cm^2) was injected into P1 segment to obtain lasing, and P2, P3, or P2 + P3 segment serves as a tuning section. The lasing wavelength of the pumped P1 segment is much larger than that of the PL peak of the material especially at the room temperature of 25 °C, and the longest lasing wavelength is ~1581.8 nm. This is because extra current is required to initiate lasing for the device consisting of unpumped segment comparing with the case of entirely pumped three segments. As discussed in Fig. 2, a higher current density leads to the band-gap shrinkage effect due to Joule heating, and the effect results in a longer lasing wavelength. Using a slightly above threshold current density of 1.34 kA/cm^2 (See Fig. 2) in the entirely pumped P1 + P2 + P3 case, the initial lasing wavelength measured is ~1549 nm and is close to the PL peak since the band-gap shrinkage effect is negligible.

Once the composite cavity laser is lasing with P1 segment pumped, wavelength tuning is achieved by current injection into the unpumped segments. A significant blue-shift of the lasing wavelength is observed at different submount temperatures (See Fig. 4). Current injection into the unpumped segments creates carriers, and the injected carriers cause changes in the absorption spectrum through band-filling, band-gap shrinkage, and free-carrier absorption effects [14]. In this case, the band-filling effect is predominant, whereby the carriers occupy states close to the bottom of the conduction band. This means those photons having energies slightly above the band-gap energy will no longer be absorbed, and the absorption at the band-gap energy decreases. Thus, electrically pumping the previously unpumped segment reduces the resonant absorption loss in the cavity, and increasing the current injection means reducing the absorption loss. As shown in Fig. 3, the peak wavelength λ_2 of the effective gain profile of the composite cavity is shifted to a shorter wavelength λ_3 and blue-shift occurs.

A change in refractive index Δn may be induced by variation in absorption $\Delta\alpha$ at any wavelength in the spectrum, and it is given by Kramers−Kronig relationship [15]

$$\Delta n(\lambda) = \frac{\lambda^2}{2\pi^2} \cdot p \cdot \int_0^\infty \frac{\Delta\alpha(\lambda_0)}{\lambda_0^2 - \lambda^2} d\lambda_0 \qquad (3)$$

where λ is the wavelength of light, λ_0 is the band-gap wavelength, and p denotes the principal value of the integral. There is a decrease in refractive index for photon energy below the band-gap energy of the unpumped segment. The band-filling effect makes the largest contribution to Δn in the composite cavity, and the lasing wavelength change is directly proportional to the relative change in the net cavity index [16].

Fig. 5 shows the temperature dependence of the wavelength-shift with P1 segment pumped above threshold and P2, P3, or P2 + P3 segment acting as the tuning section. The wavelength

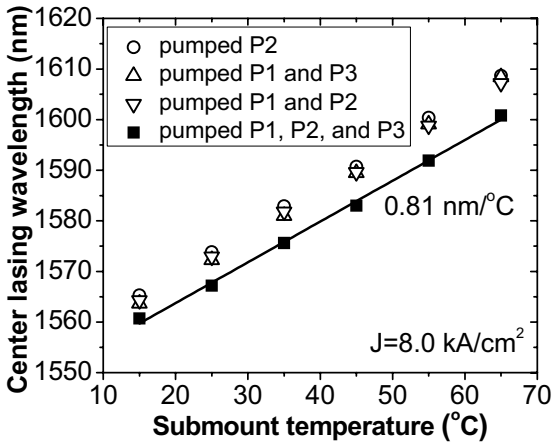

Fig. 6. Temperature dependence of center lasing wavelength for different pumped segment configurations under a constant current density at 8.0 kA/cm^2.

shift decreases with increasing submount temperature in all three cases. The shifting range also depends on the length of the previously unpumped segments. Longer unpumped segment length results in larger wavelength-shift, and the result is in agreement with the linear variation of lasing wavelength versus length of passive segment cavity in a partially pumped InGaAs/AlGaAs ridge waveguide laser [9]. At room temperature the maximum blue-shift observed in the laser device is obtained by using P2 + P3 segment as the tuning section, and the tuning range is ∼12.8 nm from 1581.8 nm to 1569 nm. The measured optical side mode suppression ratio fluctuates in the range 12.6 dB to 15.4 dB over the total tuning range, and the output power varies from ∼0.82 mW to ∼1.27 mW when the P2 + P3 segment injected total current is increased from 0 to ∼70.5 mA.

Fig. 6 shows the temperature dependence of the center lasing wavelength for different pumped segment configurations, and a constant current density at 8.0 kA/cm^2 is used for each case. The lasing wavelength shift coefficient is measured to be ∼0.81 nm/°C for the entirely pumped laser and is a typical value for quaternary III−V semiconductor QW materials [17]. For the partially pumped lasers similar coefficients are obtained and are independent of unpumped segment length. This indicates that the band-gap shrinkage effect induced by temperature shift dominates. In addition, red-shift of the lasing wavelength for partially pumped laser compared with entirely pumped laser is also observed, and the mechanism is due to the band-gap shrinkage effect as described previously.

IV. Conclusion

We have proposed, fabricated, and characterized a three-segment structure L-band wavelength-tunable MQW FP laser diode. Wavelength-tuning is achieved by electrically pumping the unpumped segments with current injection. The mechanism of wavelength-shift is investigated and explained based on carrier induced effects in semiconductors. Red-shift of the lasing wavelength is due to Joule heating and band-gap shrinkage effect. Blue-shift of the lasing wavelength is mainly caused by band-gap filling effect. At room temperature a practical tuning range is ∼12.8 nm is obtained for the device with P1 segment pumped above threshold and P2 + P3 segments as the tuning section. The tunable FP laser diode has a simple architecture and is cost effective, making them attractive for optical communication systems in the L-band wavelength.

References

[1] A. Sano, T. Kobayashi, E. Yoshida, and Y. Miyamoto, "Ultra-high capacity optical transmission technologies for 100 Tbit/s optical transport networks," *IEICE Trans. Commun.*, vol. E94B, no. 2, pp. 400–408, Feb. 2011.

[2] L. A. Coldren, "Monolithic tunable diode lasers," *IEEE J. Sel. Topics Quantum Electron.*, vol. 6, no. 6, pp. 988–999, Nov./Dec. 2000.

[3] J. Buus and E. J. Murphy, "Tunable lasers in optical networks," *J. Lightw. Technol.*, vol. 24, no. 1, pp. 5–11, Jan. 2006.

[4] T. Okamoto, *et al.*, "A monolithic wideband wavelength-tunable laser diode integrated with a ring/MZI loop filter," *IEEE J. Sel. Topics Quantum Electron.*, vol. 15, no. 3, pp. 488–493, May/Jun. 2009.

[5] Y. D. Jeong, Y. H. Won, S. O. Choi, and J. H. Yoon, "Tunable single-mode Fabry–Pérot laser diode using a built-in external cavity and its modulation characteristics," *Opt. Lett.*, vol. 31, no. 17, pp. 2586–2588, Sep. 2006.

[6] R. Phelan, *et al.*, "A novel two-section tunable discrete mode Fabry–Pérot laser exhibiting nanosecond wavelength switching," *IEEE J. Quantum Electron.*, vol. 44, nos. 3–4, pp. 331–337, Mar./Apr. 2008.

[7] N. A. Pikhtin, *et al.*, "Two-section InGaAsP/InP Fabry–Pérot laser with a 12 nm tuning range," *Tech. Phys. Lett.*, vol. 23, no. 3, pp. 214–216, Mar. 1997.

[8] J. Werner, *et al.*, "Single and double quantum well lasers with a monolithically integrated passive section," *Appl. Phys. Lett.*, vol. 57, no. 8, pp. 810–812, Aug. 1990.

[9] R. L. Williams, D. Moss, M. Dion, M. Buchanan, and K. Dzurko, "Wavelength tuning in low threshold current, partially pumped InGaAs/AlGaAs ridge waveguide lasers," *Appl. Phys. Lett.*, vol. 59, no. 22, pp. 2796–2798, Nov. 1991.

[10] J. H. Song, J. W. Park, E. D. Sim, and Y. S. Baek, "Measurements of coupling and reflection characteristics of butt-joints in passive waveguide integrated laser diodes," *IEEE Photon. Technol. Lett.*, vol. 17, no. 9, pp. 1791–1793, Sep. 2005.

[11] K. Shi, *et al.*, "Characterization of a tunable three-section slotted Fabry–Pérot laser for advanced modulation format optical transmission," *Opt. Commun.*, vol. 284, no. 6, pp. 1616–1621, Mar. 2011.

[12] T. Skettrup, "Urbach's rule derived from thermal fluctuations in the band-gap energy," *Phys. Rev. B*, vol. 18, no. 6, pp. 2622–2631, Sep. 1978.

[13] J. D. Thomson, H. D. Summers, P. M. Smowton, E. Herrmann, P. Blood, and M. Hopkinson, "Temperature dependence of the lasing wavelength of InGaAs quantum dot lasers," *J. Appl. Phys.*, vol. 90, no. 9, pp. 4859–4861, Nov. 2001.

[14] B. R. Bennett, R. A. Soref, and J. A. Del Alamo, "Carrier-induced change in reractive index of InP, GaAs, and InGaAsP," *IEEE J. Quantum Electron.*, vol. 26, no. 1, pp. 113–122, Jan. 1990.

[15] C. Thirstrup, "Refractive index modulation based on excitonic effects in GaInAs-InP coupled asymmetric quantum wells," *IEEE J. Quantum Electron.*, vol. 31, no. 6, pp. 988–996, Jun. 1995.

[16] L. A. Coldren, G. A. Fish, Y. Akulova, J. S. Barton, L. Johansson, and C. W. Coldren, "Tunable semiconductor lasers: A tutorial," *J. Lightw. Technol.*, vol. 22, no. 1, pp. 193–202, Jan. 2004.

[17] T. Higashi, T. Yamamoto, S. Ogita, and M. Kobayashi, "Experimental analysis of temperature dependence of oscillation wavelength in quantum-well FP semiconductor lasers," *IEEE J. Quantum Electron.*, vol. 34, no. 9, pp. 1680–1689, Sep. 1998.